Investigating the Usefulness of Satellite derived Fluorescence Data in Inferring Gross Primary Productivity within the Carbon Cycle Data Assimilation System

E.N. Koffi[1*], P.J. Rayner[2], A. J. Norton[2], C. Frankenberg[3], M. Scholze[4]

[1]Laboratoire des Sciences du Climat et de l'Environnement (LSCE), UMR8212, Ormes des merisiers, 91191 Gif-sur-Yvette, France

[2]School of Earth Sciences, University of Melbourne, Melbourne, Australia

[3]Jet Propulsion Laboratory, California Institute of Technology, Pasadena, USA

[4]Department of Physical Geography and Ecosystem Science, Lund University, Lund, Sweden

*now at: the European Commission Joint Research Centre, Institute for Environment and Sustainability, 21027 Ispra (Va), Italy

Correspondence to: E. N. Koffi (ernest.koffi@jrc.ec.europa.eu)

Supplementary material

Section S1: Idealized tests with SCOPE

Sensitivities of SIF and GPP to SCOPE parameters (V_{cmax}, C_{ab}, R_{in}, aPAR). The results for C4 plant are mainly shown, otherwise specified. In fact, most of the results for C3 plant are shown in the paper. The SCOPE parameters used for these simulations are given in the Table 2 of the paper, otherwise specified in the graphs or their legends.

Figure S11: Sensitivities of SCOPE SIF and GPP to V_{cmax} for various values of aPAR and for C3 plant

Figure S12: Effect of radiation on the SIF-Vcmax sensitivity and for C3 plant

Figure S13a: Sensitivities of SCOPE SIF and GPP to V_{cmax}, C_{ab}, R_{in} and for C4 plant

Figure S13b: As Figure S11, but for C4 plant

Figure S14: Sensitivities of SCOPE SIF and GPP to V_{cmax} for various values of R_{in} and aPAR and for C4 plant

C3 plant

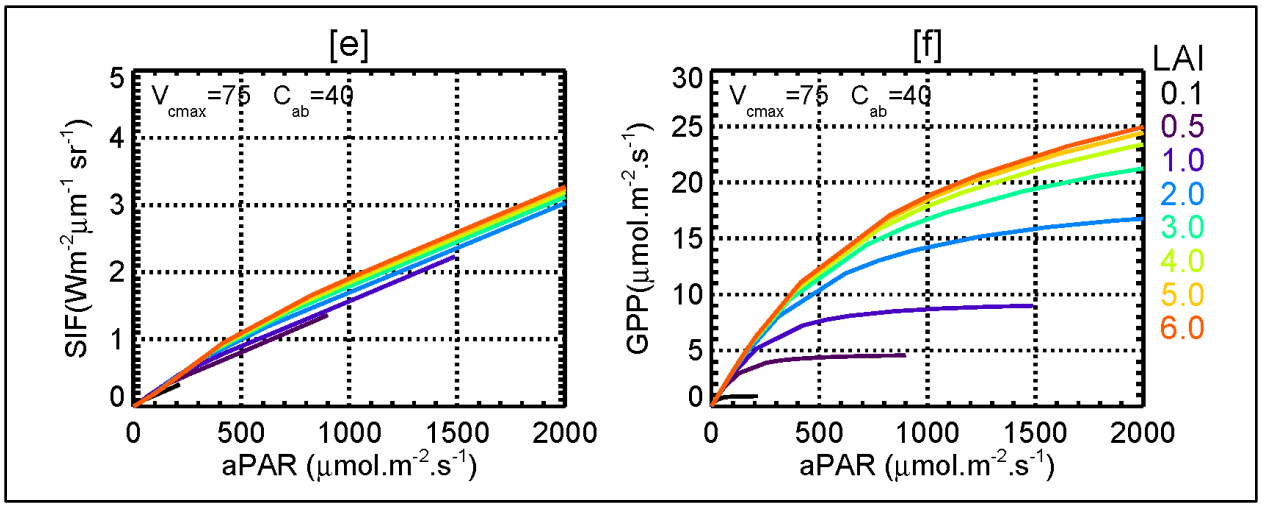

Figure S11: The sensitivities of SCOPE fluorescence SIF (e) at the top of the canopy and GPP (f) of C3 plant to absorbed phtosynthetically active radiation (aPAR) for several leaf area index (LAI) are shown. The LAI values are shown on right hand side. SIF is computed at the frequency 755 nm.

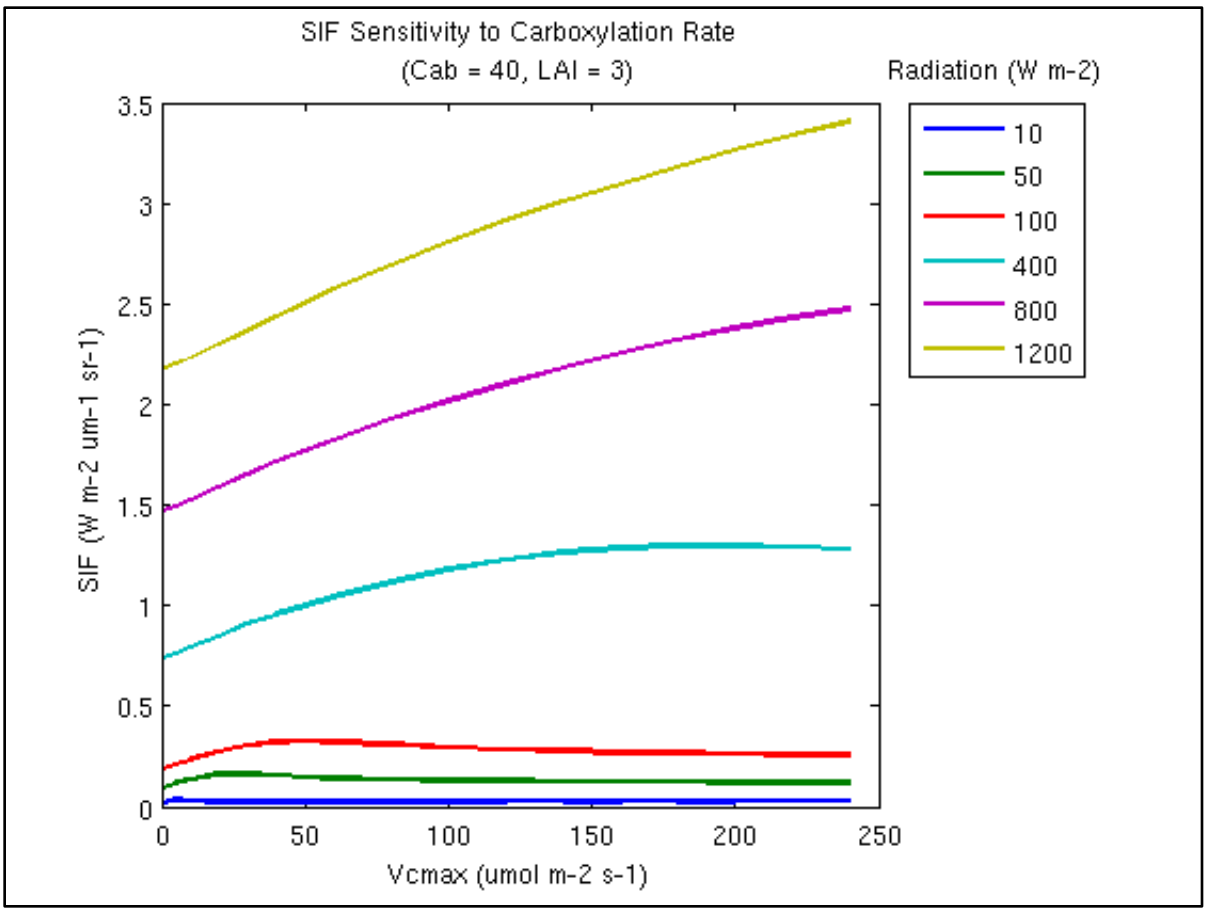

Figure S12: Effect of radiation on the SIF-Vcmax sensitivity and for C3 plant. SIF is computed at the frequency 755 nm.

C4 plant

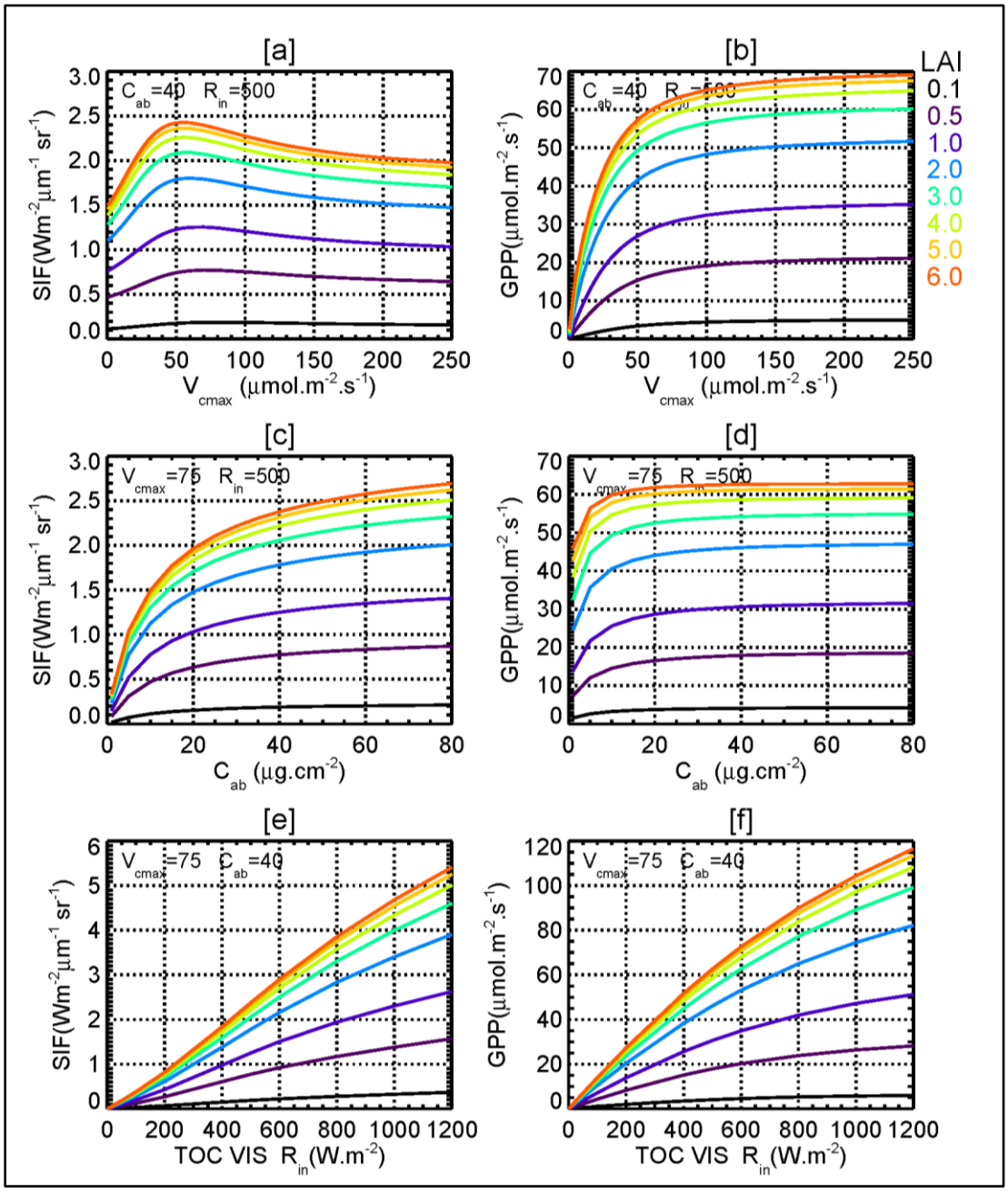

Figure S13a: The sensitivities of SCOPE fluorescence (SIF) at the top of the canopy (TOC) of C4 plant to the carboxylation maximum capacity (V_{cmax}), chlorophyll content AB (C_{ab}), and to TOC visible radiation (TOC VIS R_{in}) for several leaf area index (LAI) are shown. Graphs a) and b) stand for SIF and GPP as function of V_{cmax}, respectively. The graphs c) and d) give the sensitivities of SIF and GPP to C_{ab}, respectively. The graphs e) and f) show SIF and GPP as a function of short wave radiation at the TOC (R_{in}), respectively. The LAI values are given on the top and the right hand side. SIF is computed at the frequency 755 nm.

C4 plant

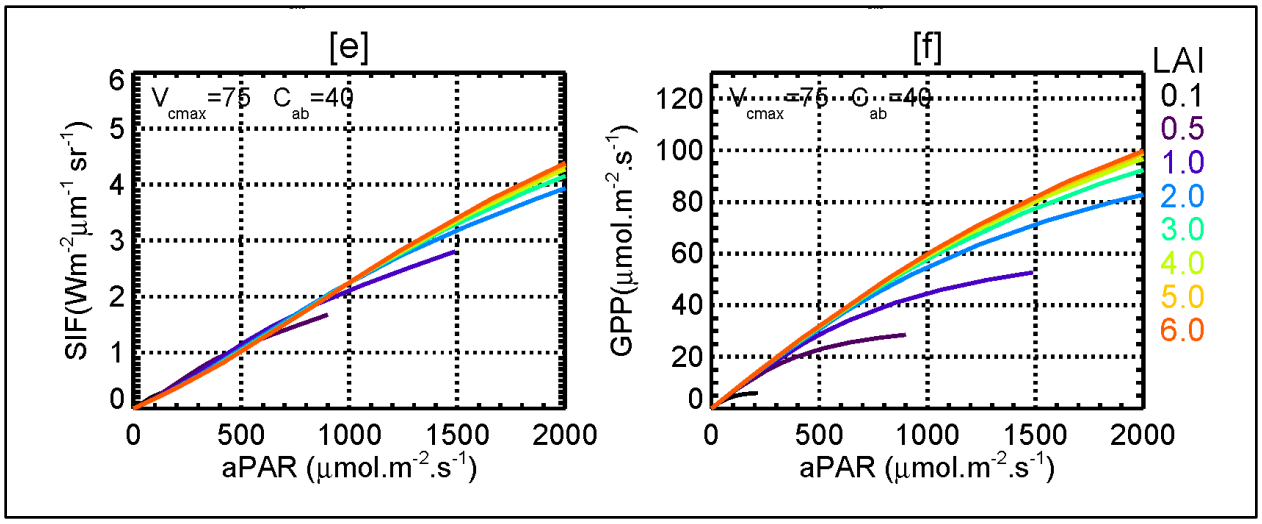

Figure S13b: The sensitivities of SCOPE fluorescence SIF (e) at the top of the canopy and GPP (f) of C4 plant to absorbed phtosynthetically active radiation (aPAR) for several leaf area index (LAI) are shown. The LAI values are given on right hand side. SIF is computed at the frequency 755 nm.

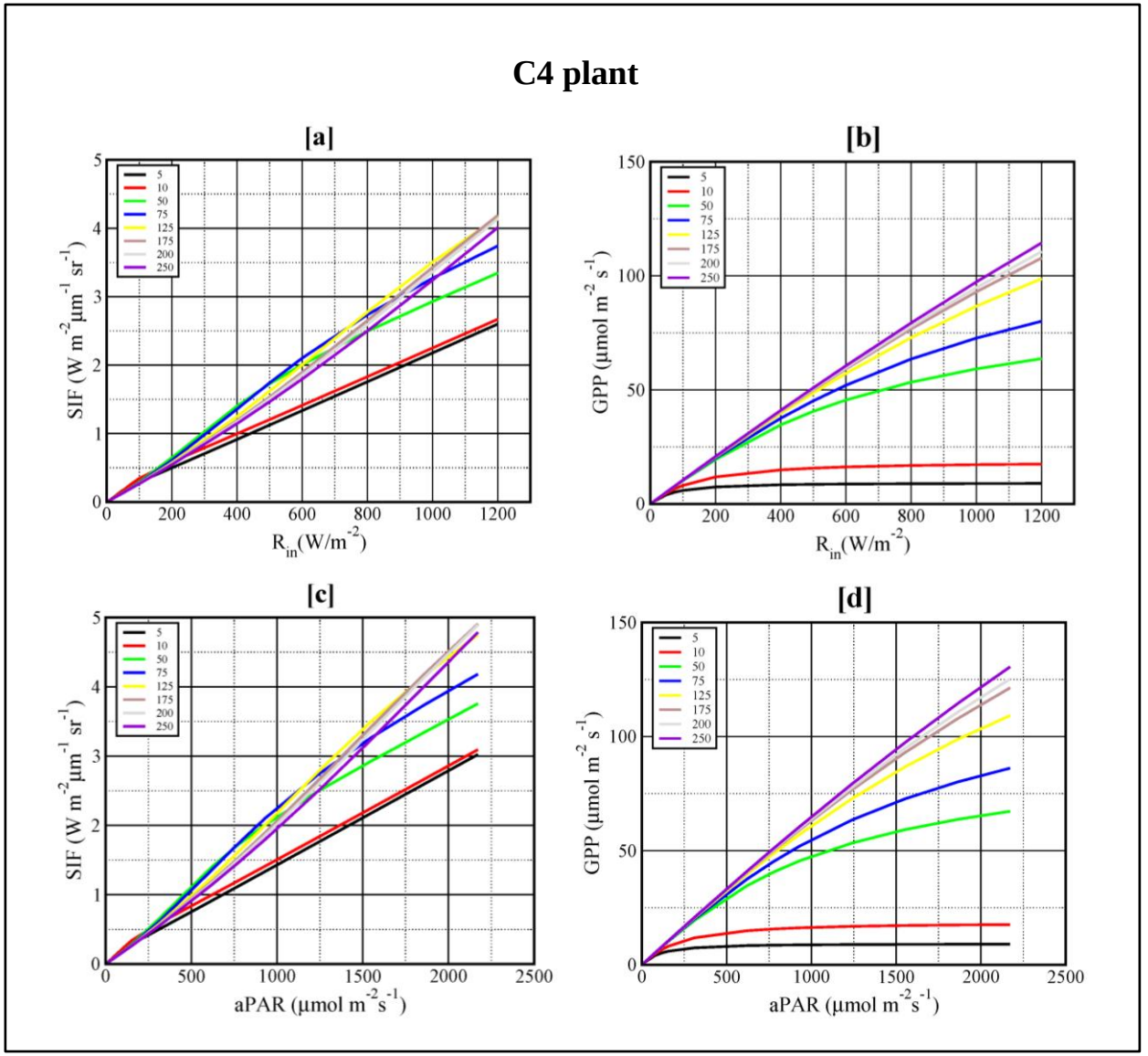

Figure S14: The sensitivities of the SCOPE fluorescence SIF (a, c) and gross primary productivity (GPP) (b, d) to the short wave radiation (R_{in}) and absorbed phtosynthetically active radiation (aPAR) and for several V_{cmax} are presented. LAI is set to 2. Results for a C4 plant are shown. The V_{cmax} values are shown in each graph. SIF is computed at the frequency 755 nm.

Section S2: Comparison of SCOPE GPP simulations to FLUXNET data

We made SCOPE simulations by using meteorological data (here temperature and incoming short wave radiation) observed at two FLUXNET stations (e.g., Baldocchi, 2003 and Papale et al., 2006; see the dedicated website: http://www.fluxnet.ornl.gov): Hyytiala (acronym FI-Hyy, longitude/latitude of 24.295^{o}/61.847^{o}*)* and Roccarespampani1 (acronym IT-Ro1 11.93/42.408). Unfortunately, we do not have any observed LAI data at these selected stations. We have then used the monthly LAIs of the biosphere model BETHY, which are relevant for the vegetation of the FLUXNET station. For this exercise, we keep constant the V_{cmax}. The V_{cmax} values are from the BETHY PFTs as given in the Table 1 of the paper. We used two V_{cmax} values: the prior and optimized values of Koffi et al. (2012). The relevant PFTs in BETHY for Hyytiala and Roccarespampani1 are 5 and 9, respectively (Table 1). The modelled GPPs are compared against the FLUXNET ones. Note that SIF data are not measured at these stations for the period examined. As an illustration of the diurnal variations of both the simulated and observed GPP together with the input variables and also the simulated SIF at the station Hyytiala during summertime are shown in **Figure 4** in the revised version of the paper. Another illustration of these diurnal variations during winter is shown in **Figure S21** for Roccarespampani1. Overall, results obtained from these two stations clearly show that SCOPE model can reproduce quite well the observed GPP with meaningful choices of both LAI and V_{cmax} values (**Figures 4** and **S21)**.

The seasonal variations of these quantities are computed for some years at each of the two selected sites and shown in **Figures S22** and **S23**. The model reproduces quite well the observed GPP. However, the simulated SCOPE GPP peak over the year occurs earlier (within 1-2 months) than observed ones. This result is maybe caused by both LAI and V_{cmax} of BETHY which seem apparently large during the growing season. Note that in these simulations, the LAIs are kept constant during a whole month and V_{cmax} is set constant for each BETHY PFT. The results of these preliminary analyses can be then reinforced by using e.g., the satellite based MODIS weekly data relevant for these stations.

Finally, these graphs also show the weak sensitivity of SIF to V_{cmax} and its relatively strong sensitivity to C_{ab}, especially under high light conditions. In contrary, SCOPE GPP is insensitive to C_{ab}, but strongly sensitive to V_{cmax} (**Figures 4, S21, S22,** and **S23**).

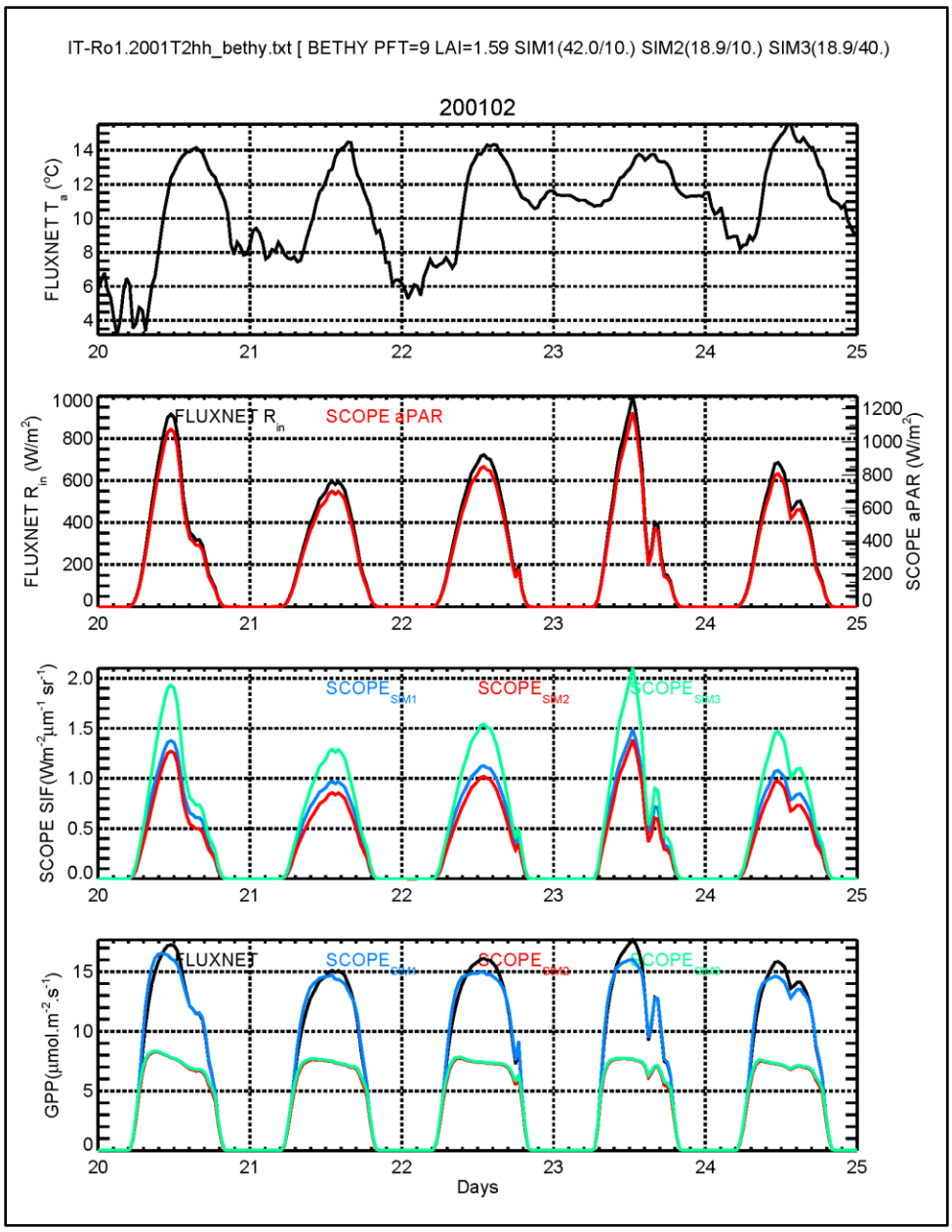

Figure S21: SCOPE simulations of SIF, GPP, and aPAR from in situ measurements at Roccarespampani1 (acronym IT-Ro1 with longitude/latitude of 11.93/42.408) in Italy during 2001 over 20 to 25 February period. The graph a) presents the temporal variations of the observed temperature. Graph b) shows the temporal variations of both observed short wave radiation R_{in} (black) and SCOPE simulated aPAR (red). Graphs c and d) display the simulated SIF and GPP by using two values of both V_{cmax} and C_{ab} (blue: $SCOPE_{SIM1}$: V_{cmax}/C_{ab} = 42 µmol m^{-2} s^{-1}/10 µg cm^{-2}; red: $SCOPE_{SIM2}$: 18.9/10.; green: $SCOPE_{SIM3}$: 18.9/40.). The FLUXNET observed GPP is shown in graph d) and in black. The other SCOPE parameters are given in Table 2. The C3 plant is considered in SCOPE model. SIF is computed at the frequency 755 nm.

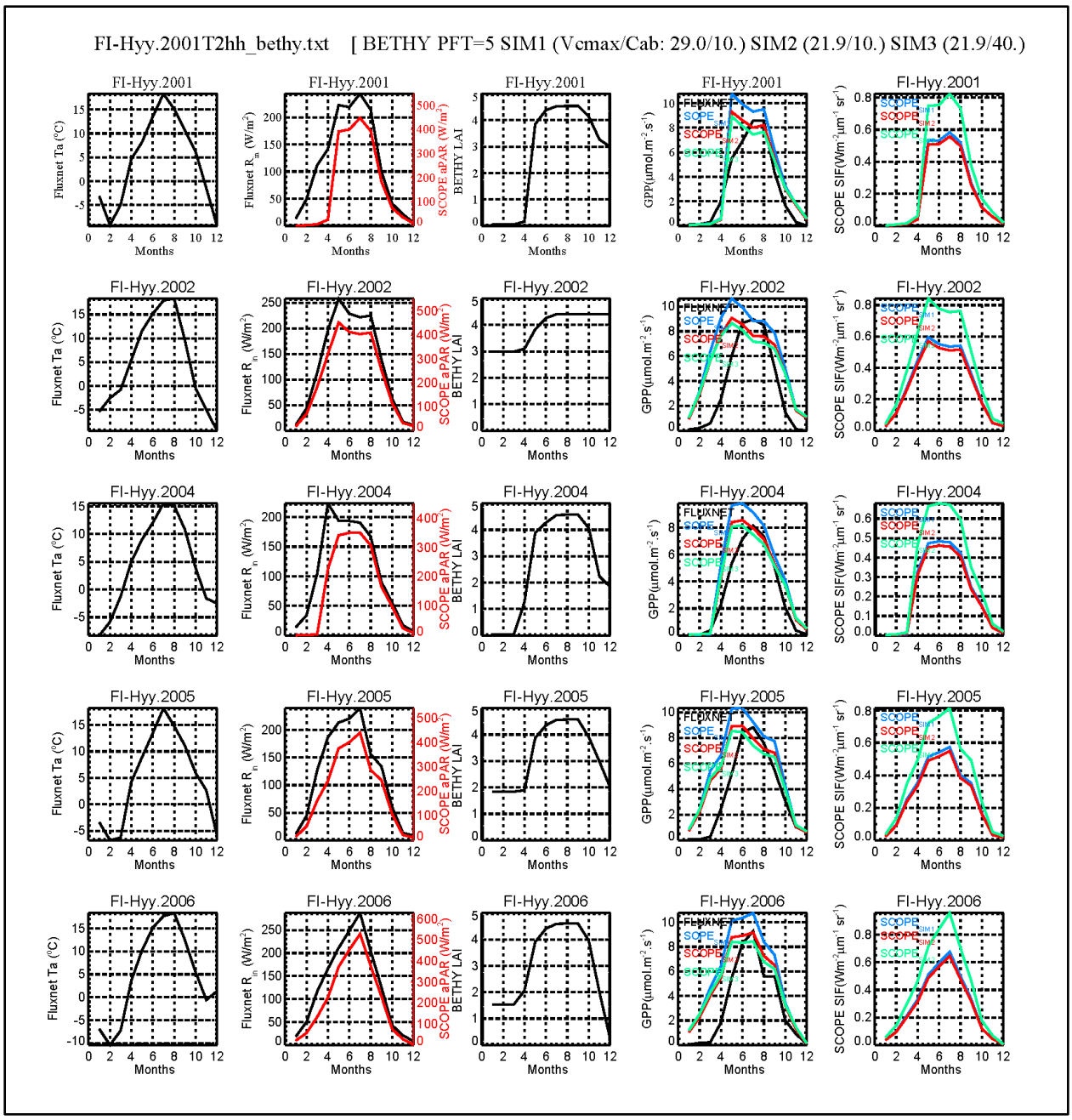

Figure S22: Seasonal variations of FLUNET data (here temperature T_a, short wave radiation R_{in}, and GPP) and SCOPE simulated quantities (aPAR, GPP, and SIF) at Hyytiala (acronym FI-Hyy and having longitude/latitude of 24.295°/61.847°) by using BETHY monthly LAI relevant to the vegetation of the station. The simulated SIF and GPP are performed by using two values of both V_{cmax} and C_{ab} (blue: $SCOPE_{SIM1}$: V_{cmax}/C_{ab} = 29 μmol m^{-2} s^{-1}/10 μg cm^{-2}; red: $SCOPE_{SIM2}$: 21.9/10; green: $SCOPE_{SIM3}$: 21.9/40). The observations are in black and simulations in colors. SIF is computed at the frequency 755 nm.

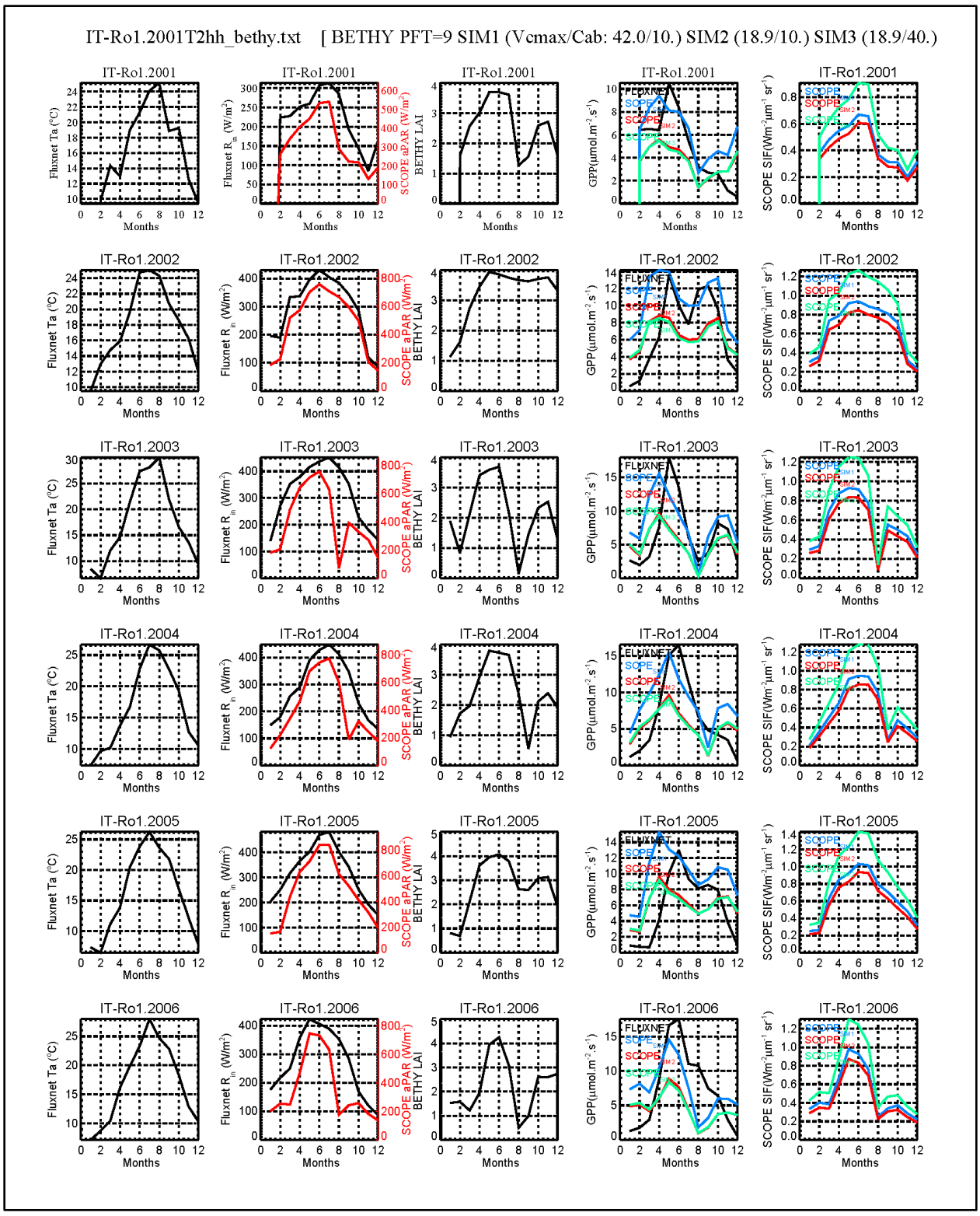

Figure S23: As Figure S22, but at Roccarespampani1 (acronym IT-Ro1) FLUXNET station. The values of V_{cmax} and C_{ab} for SCOPE simulations are given on the top of the graph

Section 3: CCDAS simulations

Figure S31: Seasonal variations of the range of short wave radiation values R_{in} used in the CCDAS simulations and for 2010 and at global and regional (southern hemisphere SH; Tropics; northern hemisphere NH) are shown.

Figure S32: Seasonal variations of SIF and aPAR for different regions of the globe

Figure S33: Latitudinal distributions of SIF and aPAR

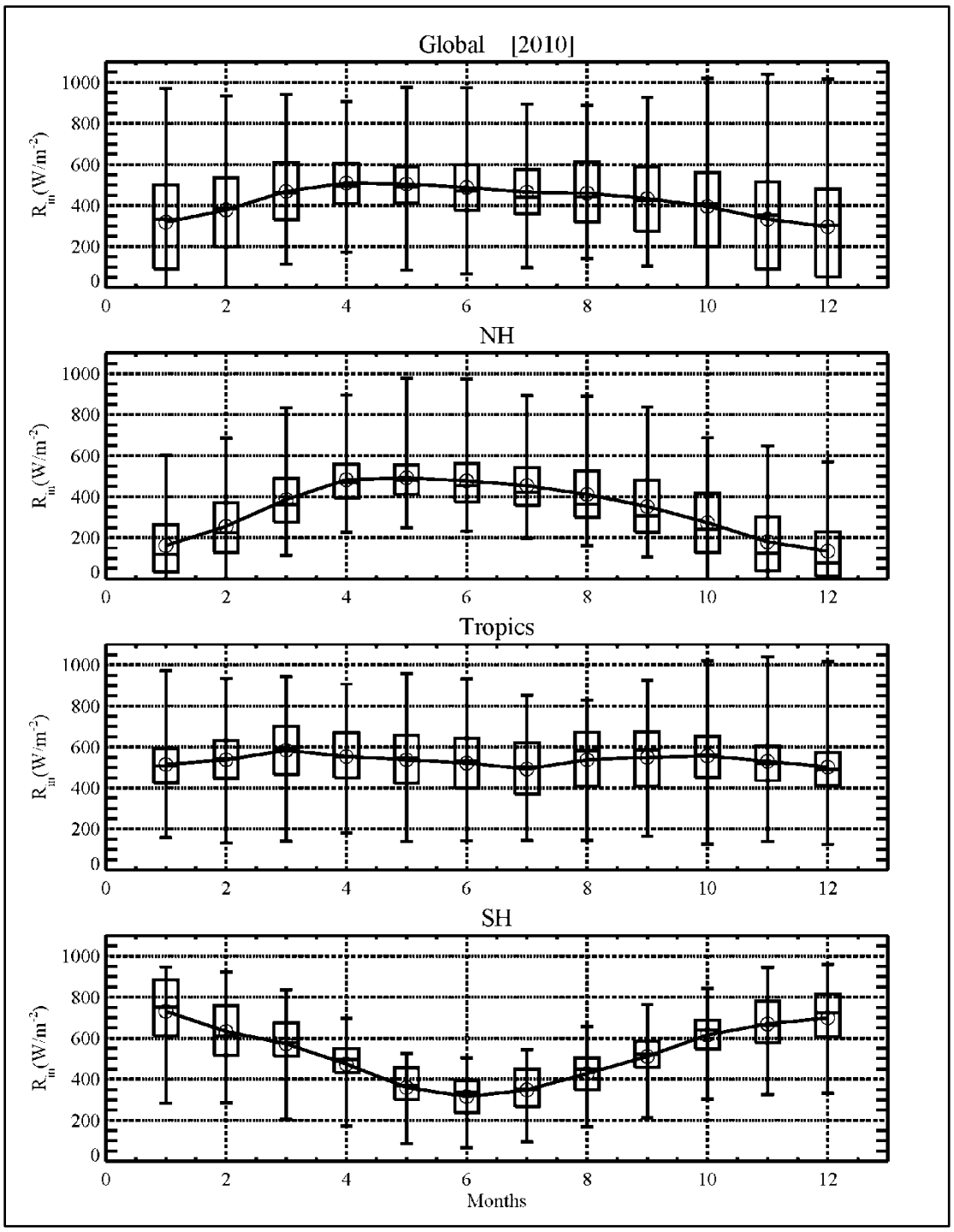

Figure S31: Seasonal variations of the range of monthly short wave radiation values R_{in} used in the CCDAS simulations and for 2010 and at global and regional (Northern Hemisphere NH; Tropics; Southern Hemisphere SH) scales are shown. The minimum and maximum values of each month are shown. The boxes are delimited by the 25% and 75% percentiles. The median values are given by the horizontal line in the boxes. The mean values are given by the open circles

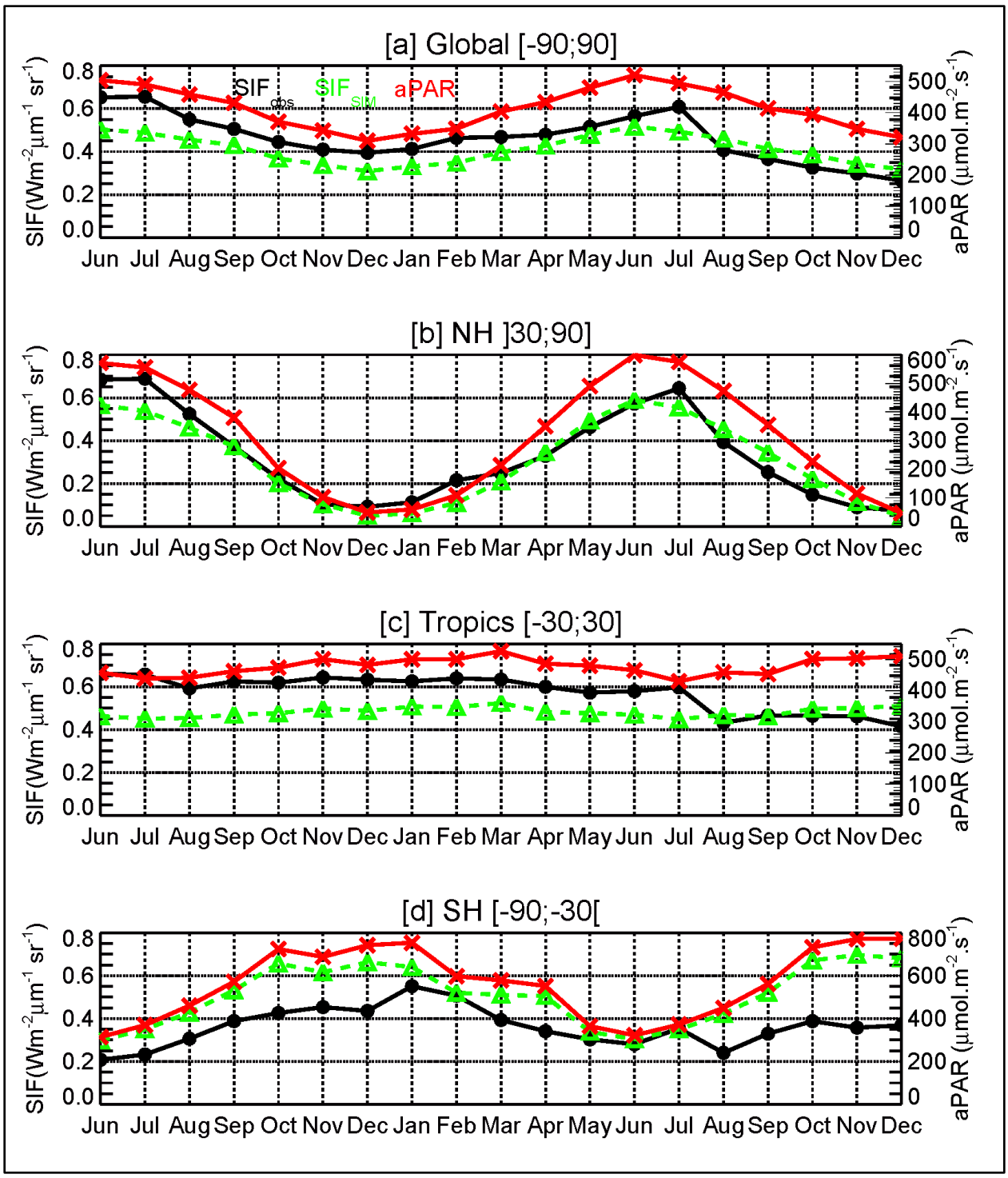

Figure S32: Global (a) and regional (b to d) means of fluorescence SIF and absorbed phtosynthetically active radiation (aPAR) over June 2009 to December 2010 period are shown. The satellite GOSAT based SIF (SIF_{OBS}: black solid line with big dot), simulated SIF (SIF_{SIM}: green dashed line with triangles), and the simulated gross primary productivity (aPAR: red solid line with crosses) are displayed. The CCDAS set up S4 (Table 3) is considered.

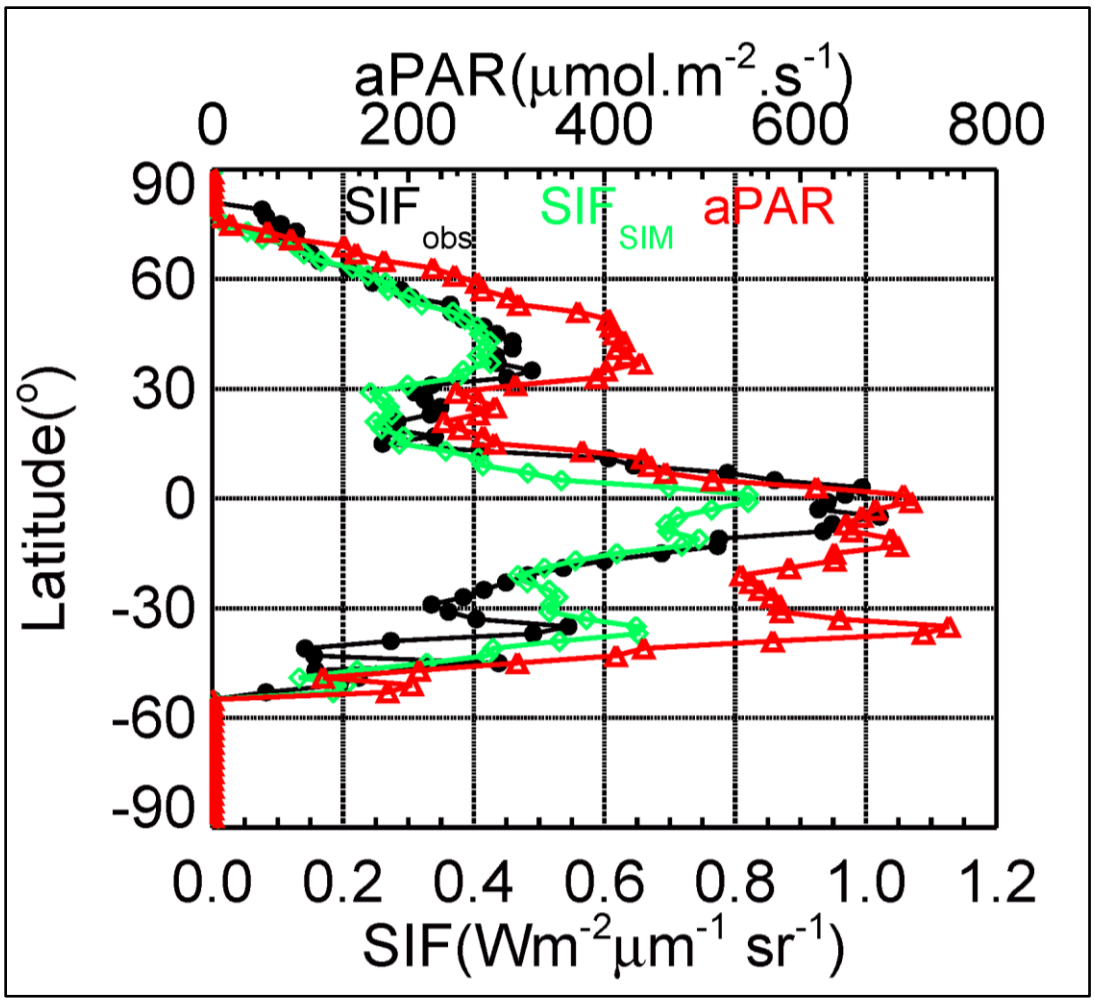

Figure S33: Latitudinal distributions of the satellite GOSAT based SIF (SIF_{OBS}: black solid line with big dot), simulated SIF (SIF_{SIM}: green solid line with diamonds), and absorbed phtosynthetically active radiation (aPAR: red solid line with triangles) within 5° latitudinal band are shown. The CCDAS set up S4 (Table 3) is considered. The period of June 2009 and December 2010 period is considered.

Section S4: Simulations of Zhang et al. (2014) with SCOPE v1.53

To understand the differences between our results and those from Zhang et al. (2014), we carefully made detailed analysis by using the SCOPE model alone and SCOPE settings reported in Zhang et al. (2014). For the environmental input (temperature and short wave radiation), we used their values over a large range. Then, we made simulations of SIF at ecosystem by using the C4 crop (here corn and soybean) with SIF retrieved at the frequency 740 nm. The tests are carried out by using the SCOPE model alone with the fluorescence model choice "0" (i.e., empirical fit to Flexas'data; version 1.53). In details, the more relevant settings of SCOPE we used can be described as follows. The radiation varies from 1 to 1200 W/m^2. The V_{cmax} varies from 1 to 350 μmol m^{-2} s^{-1}. The temperature varies from 10°C to 30°C. C_{ab} values from 1 to 80 μg cm^{-2} are used. Several values of LAI (between 0.1 and 6) are used. The strongest sensitivity for SIF was found for a temperature input of 28°C, a LAI of 6 (**Figure S41**). This optimal simulation sensitivity does not reach the magnitude seen in Zhang et al. (2014). Using these inputs, SIF almost double between V_{cmax} values of 10 and 200, whereas Zhang et al. (2014) sees SIF increases by a factor greater than three (See Figure 3 in Zhang et al., 2014). Again, with the current version of SCOPE we are using, we do not find such a strong sensitivity of SIF to V_{cmax} as obtained from Zhang et al. (2014). Our results do show a weak sensitivity of SIF to V_{cmax} under low light condition and this sensitivity slightly increases with the increase of the radiation when, but only for a rapid increase of V_{cmax} (e.g., between 10 and 75μmol m^{-2} s^{-1}) relative to growing period of the studied crops (**Figure S41**).

The sensitivities of SIF to both C_ab and LAI are also shown in **Figure S41**. As expected, results clearly show the large sensitivity of SIF to these parameters.

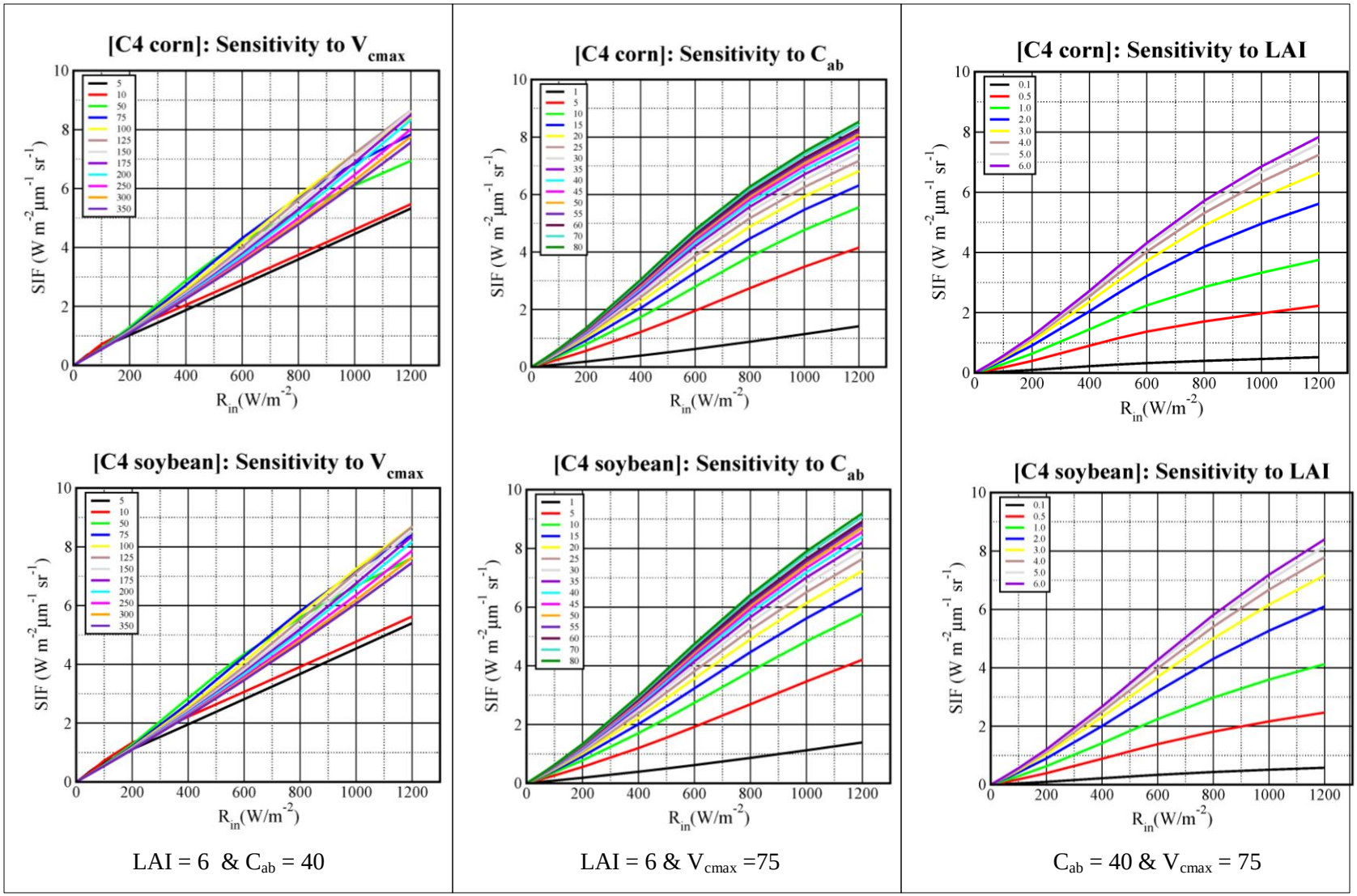

Figure S41: Sensitivity of SIF to V_{cmax}, C_{ab}, and LAI as a function of the short wave radiation (R_{in}). SIF is computed at the frequency 740 nm. The other SCOPE parameters are given in Table 2 of the paper. The Ball-Berry stomatal conductance parameter m in SCOPE model is set to 4 for corn and 9 for soybean, respectively. The temperature is set to 28°C. SIF is computed at the frequency 740 nm.

Acknowledgment
We are grateful to both Timo Vesala and Dario Papale for providing FLUXNET data at the stations Hyytiala and Roccarespampani 1, respectively.

References

Baldocchi, D. D. (2003), Assessing the eddy covariance technique for evaluating carbon dioxide exchange rates of ecosystems: past, present and future. Global Change Biology, 9, 479–492.

Papale D., Reichstein, M., Aubinet, M., Canfora, E., Bernhofer, C., Kutsch, W., Longdoz, B., Rambal, S., Valentini, R., Vesala, T., and Yakir, D.: Towards a standardized processing of Net Ecosystem Exchange measured with eddy covariance technique: algorithms and uncertainty estimation. Biogeosciences, 3, 571–583, 2006.